Green and Efficient Construction of imidazo[2,1-*b*][1,3,4]thiadiazoles using Lanthanide Doped Magnesium Ferrite Nanoparticals through Multicomponenet GBB annulation

Dr. Anamika Prajapati[1]*, Umesh Chejara[2]

1 Assistant Professor, Department of Chemistry, Government Science College, Sikar, Rajasthan, India

aonu27@gmail.com

2 Lecturer, Department of Physics, PM SHRI MGGS Jeeni, Surajgarh, Jhunjhunu, Rajasthan, India

Abstract: lanthanide doped magnesium ferrite nanoparticles act as highly efficient heterogeneous catalysts in the Groebke–Blackburn–Bienaymé (GBB) Synthetic approach, promoting the annulation of 2-amino-1,3,4-thiadiazole with isocyanides and aldehydes to synthesize imidazo[2,1-b][1,3,4]thiadiazoles and bond-forming efficiency and procedural simplicity, enabling the rapid and economical construction of complex bioactive and structurally diverse molecular scaffolds.. Under the optimized conditions, 10 mol% $MgCe_{0.4}Er_{0.6}FeO_4$ in dichloromethane at 50 °C afforded the model product in 94% isolated yield within 40 min. The catalyst could be separated readily and reused for six consecutive cycles (with isolated yields of 94, 94, 92, 92, 90 and 87%, respectively) thereby making the process economically viable, eco-compatible for large-scale and industrial implementation. The protocol also provided a series of imidazothiadiazole derivatives in good to excellent yields. UV–Visible, FT-IR, XRD and SEM measurements were used to characterize the prepared nanomaterial.

Keyword: lanthanide doped magnesium ferrite; $MgCe_{0.4}Er_{0.6}FeO_4$; nanopartical; Groebke–Blackburn–Bienaymé reaction; imidazo[2,1-*b*][1,3,4]thiadiazole

INTRODUCTION

The development of novel heterocyclic scaffolds from simple building blocks through energy-efficient and environmentally benign combinational chemistry has attracted significant interest

in molecular synthesis and drug discovery. [1] Isocyanides functional group exhibit unique and versatile reactivity.

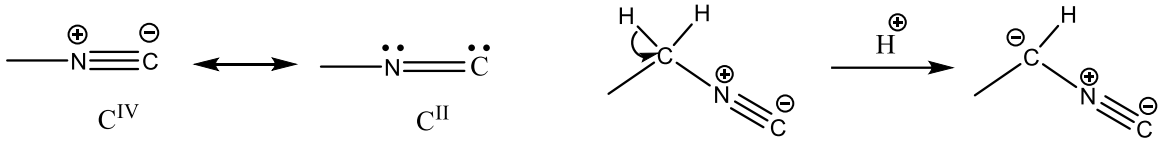

(a) C^{IV} resonates with the C^{II} form (b) Isocyanide shows α-acidity like carbonyl

Scheme1: Showing isocyanide functional group reactivity

Isocyanides can react with both nucleophiles and electrophiles at the same carbon center. The chemistry of isocyanides is characterized by three properties: the α-acidity, the α-addition and the easy formation of radicals. (Scheme [1])

Among isocyanide-based multicomponent processes, the Groebke–Blackburn–Bienaymé (GBB) approach offers a direct route to nitrogen-containing heterocyclic frameworks through the combination of an amino component, a carbonyl compound and an isocyanide. Such transformations are attractive due to several structural modification can be incorporated in one operation while avoiding lengthy sequences of separate functional-group manipulations. Nanoparticle-supported catalytic systems have further expanded the applicability of multicomponent GBB reactions by providing heterogeneous surfaces with accessible catalytic sites. These sustainable approaches facilitate easy separation, catalyst recovery and reuse, while reducing waste generation under mild reaction conditions. [6]

Diverse range of catalysts have been used to catalyze Groebke–Blackburn–Bienaymé (GBB) reaction by Lewis acids such as $SnCl_2$[7a], $Cu(OTf)_2$ [7b], $Sc(OTf)_3$ [7c], $In(OTf)_3$ [7d, 7e], $In(OTf)_3$-HBF_4 [7f], $La(OTf)_3$ [7g], $RuCl_3$[7h], $LaCl_3.7H_2O$ [7i], $ZnCl_2$ [7j], $ZrCl_4$ [7k], and other such as Cs_2CO_3 [8a], NH_4Cl [8b], acetic acid [8c], perchloric acid [8d], tosylic acid [8e], silicasulfuric acid [8f].

Imidazo[2,1-b][1,3,4]thiadiazoles represent a promising class of bioactive heterocycles owing to their significant pharmaceutical and therapeutic potential such as antibacterial, antifungal, anticancer, and anticonvulsant activities, potent tumor associated human carbonic anhydrase IX and XII inhibitors. Their distinctive structural features, including four heteroatoms, two fused privileged heterocyclic systems, and extended π-conjugation, contribute to their diverse biological activities. Notably, the imidazothiadiazole scaffold is incorporated into the structures of several bioactive natural products and synthetic pharmaceuticals (Figure 1). [9a-9f]

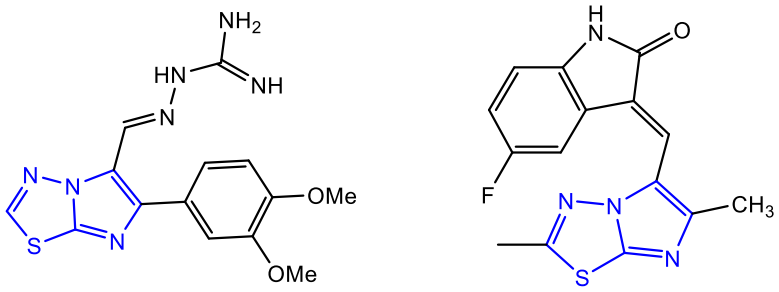

imidazothiazole guanylhydrazone derivative imidazothiadiazole–oxindole

Figure 1: Bioactive molecules containing thiadiazole moeity.

In the present work examines the use of lanthanide doped magnesium ferrite nanoparticles ($MgCe_{0.4}Er_{0.6}FeO_4$) in a three-component GBB reaction involving 2-amino-1,3,4-thiadiazole, isocyanides and diverse aldehydes building blocks under mild reaction conditions. The catalytic protocol was optimized using a model reaction, followed by substrate-scope studies and evaluation of catalyst recovery and reuse.

RESULTS AND DISCUSSION

A model transformation was selected to establish suitable conditions for the GBB annulation. 2-amino-1,3,4-thiadiazole, tert-butyl isocyanide and thiophene-2-carbaldehyde were reacted in the presence of $MgCe_{0.4}Er_{0.6}FeO_4$ nanoparticles. The optimized experiment employed 10 mol% catalyst in DCM at 50 °C and produced the desired imidazothiadiazole in 94% isolated yield after 40 min (Scheme 2).

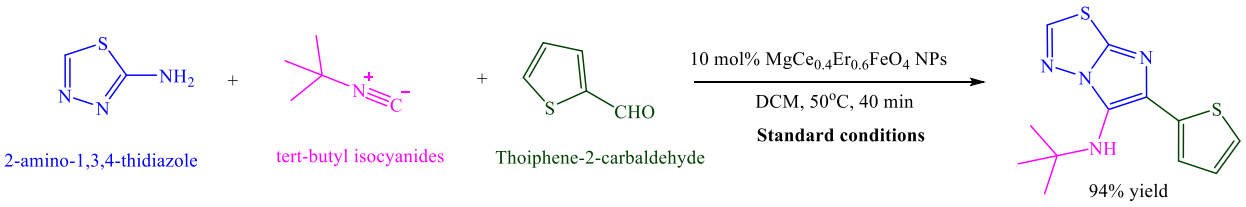

Scheme 2: Model reaction

Table 1: Optimization studies

Entry	Deviation from standard conditions[a]	Yield(%)[c]
1.	No catalyst	trace
2.	Ethanol instead of DCM	75[b]
3.	THF instead of DCM	86[b]
4.	Diethyl ether instead of DCM	62[b]
5.	80°C instead of 50°C	89
5.	$In(OTf)_3$ instead of $MgCe_{0.4}Er_{0.6}FeO_4$ NPs	75[d]
6.	Trifluoroacetic acid instead of $MgCe_{0.4}Er_{0.6}FeO_4$ NPs	72[d]
7.	PTSA instead of $MgCe_{0.4}Er_{0.6}FeO_4$ NPs	62[d]
8.	$MgFe_2O_4$ instead of $MgCe_{0.4}Er_{0.6}FeO_4$ NPs	80

[a] All the reactions were carried out using 2-amino-1,3,4-thidiazole (0.30 mmol), tert-butyl isocyanides (0.30 mmol) and Thoiphene-2-carbaldehyde (0.30 mmol) using 10 mol% catalyst in appropriate solvent (0.2M concentration) and stirred till completion, as indicated by TLC.

[b] 80% completion after 2h

[c] Isolated yield after purification.

[d] 80°C, 12h

The importance of the catalyst was first examined by carrying out the model reaction without $MgCe_{0.4}Er_{0.6}FeO_4$ NPs. Only trace product formation was observed, showing that the nanoferrite substantially promotes the transformation. The solvent was then varied. Replacement of DCM by ethanol, THF or diethyl ether gave yields of 75%, 86% and 62%, respectively. These observations identified DCM as the most suitable solvent among those examined.

Temperature variation was subsequently investigated. Raising the temperature from 50 to 80 °C gave an 89% yield after 40 min, which was still lower than the 94% obtained at 50 °C. The

$MgCe_{0.4}Er_{0.6}FeO_4$ catalyst was also compared with selected conventional catalytic systems. $In(OTf)_3$ and trifluoroacetic acid afforded 75% and 72% yields, respectively, while p-toluenesulfonic acid provided 62% yield. Undoped $MgFe_2O_4$ nanoparticles gave an 80% yield under the corresponding conditions. The Ce/Er-doped material therefore gave the highest yield in the examined series.

The superior performance of the doped ferrite may be associated with changes in surface characteristics and the availability of catalytically active sites produced by lanthanide substitution. On the basis of the optimization experiments, $MgCe_{0.4}Er_{0.6}FeO_4$ NPs (10 mol%) in DCM at 50 °C was selected as the standard condition for subsequent reactions. The complete optimization data should be retained as Table 1.

The reusability of $MgCe_{0.4}Er_{0.6}FeO_4$ NPs was assessed with the model reaction under the selected standard conditions. Following completion, the solid catalyst was isolated by filtration, washed three times with diethyl ether to remove retained organic material, dried under vacuum and subsequently oven-dried. The recovered material was then introduced into the next reaction cycle.

The catalyst remained active through six consecutive runs. The isolated yields recorded for cycles 1–6 were 94%, 94%, 92%, 92%, 90% and 87%, respectively. Thus, although a gradual decline in yield was observed over repeated use, the catalyst retained substantial activity throughout the six-cycle experiment. The recycling profile is presented in Figure 2.

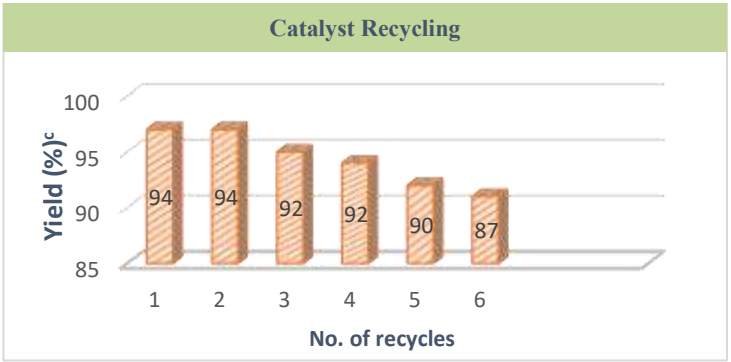

Figure 2: Recyclability and reusability of $MgCe_{0.4}Er_{0.6}FeO_4$ NPs.

The prepared $MgCe_{0.4}Er_{0.6}FeO_4$ material was examined using complementary spectroscopic and microscopic techniques. In the UV–Visible spectrum, the nanoferrite showed a maximum absorption at approximately 222 nm. [Figure 3(a)] The FT-IR spectrum recorded between 400

and 4000 cm^{-1} displayed characteristic metal–oxygen vibrations associated with the ferrite framework. Bands near 561 and 437 cm^{-1} were assigned to metal–oxygen vibrations at tetrahedral and octahedral sites, respectively. Additional absorptions in the 1544–1549, 1404 and 1107–1147 cm^{-1} regions were attributed to O–H, C=O and nitrate-related vibrations, respectively. [Figure 3(b)]

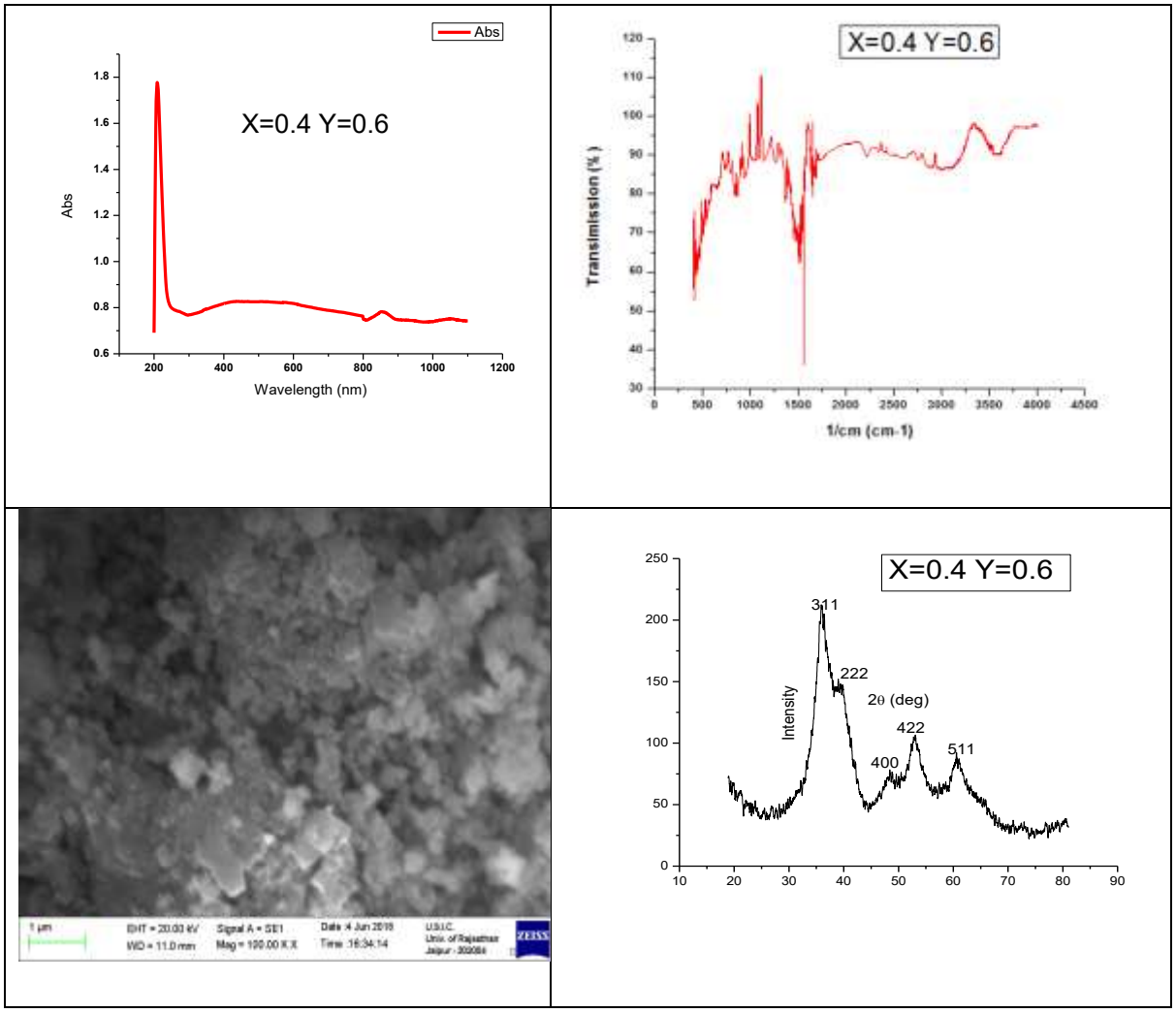

Figure 3 (a) Showing UV-Vis absorption spectrum of $MgCe_{0.4}Er_{0.6}FeO_4$ nanoparticles (b) Showing FT-IR spectrum of $MgCe_{0.4}Er_{0.6}FeO_4$ nanoparticles (c) Showing XRD of $MgCe_{0.4}Er_{0.6}FeO_4$ nanoparticles (d) Showing SEM of $MgCe_{0.4}Er_{0.6}FeO_4$ nanoparticles

Powder X-ray diffraction measurements were carried out with Cu Kα radiation (λ = 1.5406 Å). Reflections assigned to the (220), (311), (400) and (422) planes were observed, consistent with the reported spinel ferrite structure. The dominant (311) reflection was used with the Scherrer equation to estimate crystallite size. For $MgCe_{0.4}Er_{0.6}FeO_4$, the reported average crystallite size was approximately 1.31 nm. The manuscript attributes changes in lattice

parameters after Ce^{3+}/Er^{3+} substitution to differences in ionic radii and the preferential occupation of tetrahedral and octahedral positions. [Figure 3(c)]

SEM examination showed relatively uniform nanoparticles accompanied by some agglomeration. The particles displayed an approximately cubic morphology and dimensions below 40 nm. [Figure 3(d)] These observations were reported to be consistent with the nanoscale character indicated by the XRD analysis. The original UV–Visible, FT-IR, XRD and SEM plots should be retained as Figure 3.

Under the optimized reaction conditions, the isocyanide based three- component reaction was extended for the synthesis of structurally diverse imidazothiadiazoles to explore the scope and generality of the reaction protocol. To our delight, the reaction proceeds smoothly and the structurally diverse imidazothiadiazoles were obtained in excellent yields. The results are summarized in Scheme 3.

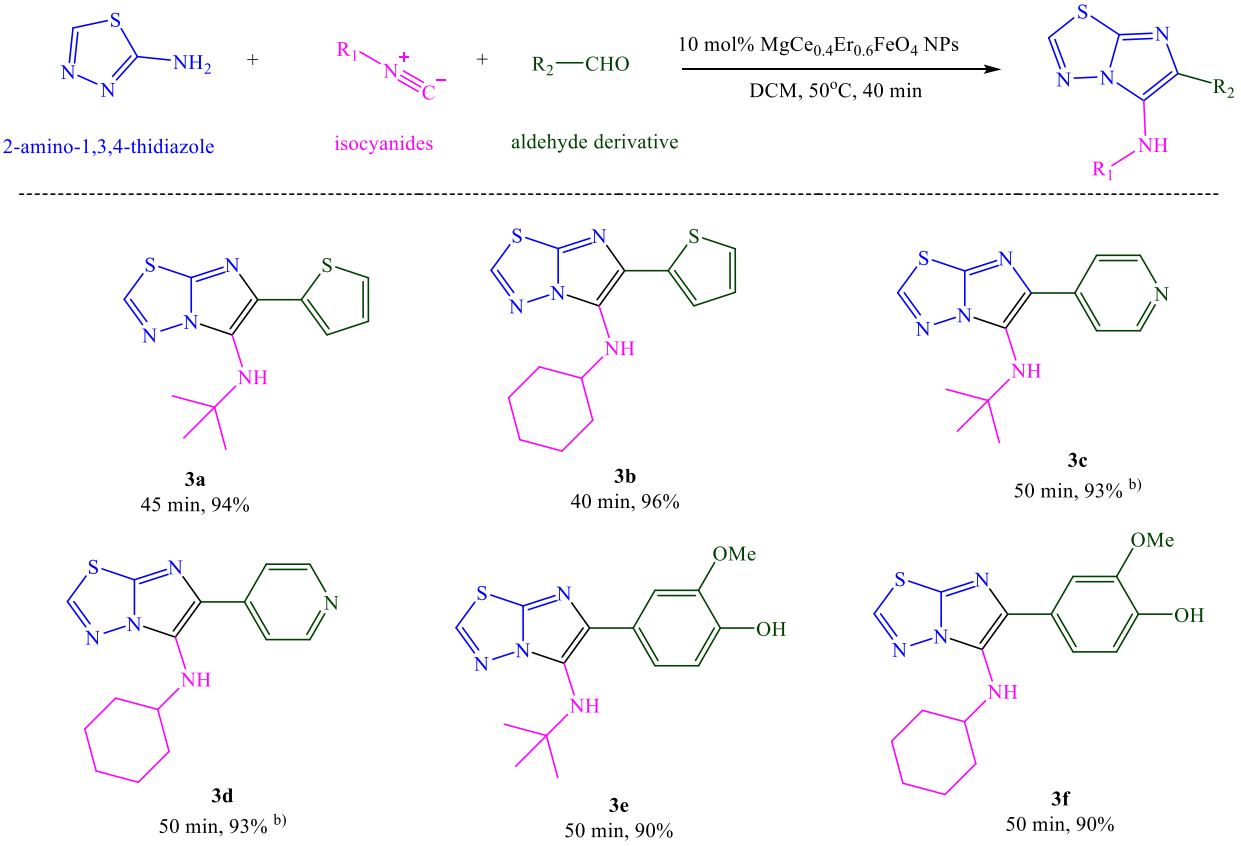

Scheme 3: Synthesis of imidazothiadiazole derivatives[a]

[a] Reaction conditions: 2-amino-1,3,4-thiadiazole (1 mmol), cycohexyl/tert.butyl isocyanides (1 mmol), and thiophene-2-carbaldehyde/4-pyridinecarboxaldehyde/4-hydroxy-3-

methoxybenzaldehyde (1 mmol); catalyst: $MgCe_{0.4}Er_{0.6}FeO_4$ NPs (10 mol%); Solvent: (0.2M concentration) ; Temperature: 50°C and stirred till completion, as indicated by TLC.

[b] 15 mol% $MgCe_xEr_yFe_{2-x-y}O_4$ NPs at 70°C.

A plausible pathway for formation of the imidazothiadiazole products is illustrated in Scheme 4. The proposed sequence begins with activation of the aldehyde carbonyl group by $MgCe_{0.4}Er_{0.6}FeO_4$, followed by condensation with 2-amino-1,3,4-thiadiazole to generate the corresponding imine intermediate. Reaction of this intermediate with tert-butyl isocyanide can then proceed through two suggested routes.

In pathway A, the isocyanide participates in a [4+1] cycloaddition. In the alternative pathway B, α-isocyanide addition is followed by 5-exo-dig cyclization and a subsequent 1,3-H shift, leading to the fused heterocyclic product. The nanoferrite $MgCe_{0.4}Er_{0.6}FeO_4$ is proposed to assist the sequence through surface sites capable of activating and stabilizing reaction intermediates. These pathways are presented as plausible mechanistic interpretations rather than experimentally established elementary steps.

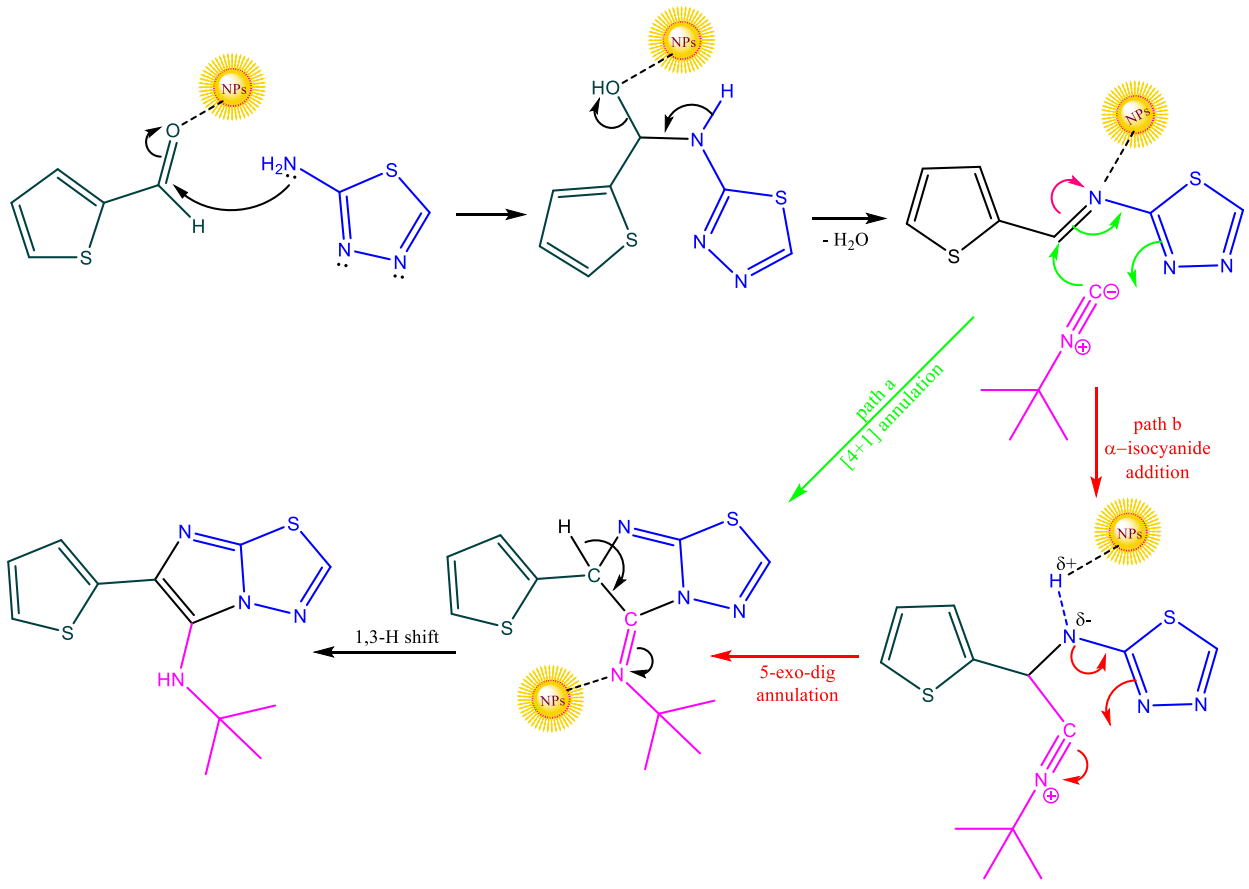

Scheme 4: Plausible reaction mechanism

The $MgCe_{0.4}Er_{0.6}FeO_4$ nanoparticles play a crucial catalytic role by providing accessible surface-active sites for the activation and stabilization of reaction intermediates, thereby promoting the sequential bond-forming steps under mild conditions.

Synthesis of $MgCe_{0.4}Er_{0.6}FeO_4$ Nanoparticles

Controlled synthesis is crucial for lanthanide doped magnesium ferrite nanoparticles we use the sol–gel auto-combustion route offers good compositional homogeneity, low energy consumption. Accordingly, Ce^{3+}- and Er^{3+}-substituted magnesium ferrite nanoparticles with the general composition $MgCe_xEr_yFe_{2-x-y}O_4$ (x = 0.4 y = 0.6) were synthesized by this method. Stoichiometric amounts of $Mg(NO_3)_2{\cdot}6H_2O$, $Fe(NO_3)_3{\cdot}9H_2O$, $[Ce(NO_3)_2.6H_2O]$ and $[Er(NO_3)_3.5H_2O]$ precursors were dissolved in double-distilled water, followed by the addition of citric acid as a complexing/fuel agent. The resulting solution was stirred and heated at 80 °C, and its pH was adjusted to 7 using aqueous ammonia. Subsequent heating at 100–140 °C produced a viscous gel, which underwent self-propagating combustion to yield a voluminous powder. The obtained powder was ground and calcined at 220 °C for 4 h to obtain the desired spinel ferrite phase.

Compounds names and spectral details:

5- (tertiarybutylamino) -6- (pyridin-4-yl) imidazo [2,1-b] [1,3,4] thiadiazole (3c): M.p. 125-127°C. IR (KBr) (ν_{max} cm^{-1}):. 3299, 3050, 2945, 2930, 1580, 1530, 1492, 1470, 1421, 1348, 1055, 905, 720, 645. ^{1}H NMR (DMSO-d^6) δ (ppm): 1.02 (s, 9H, CH_3), 4.55 (Br s, 1H, NH), 7.99-8.95 (m, 5H, ArH). ^{13}C NMR (DMSO-d^6) δ(ppm): 30.2, 56.1, 121.3, 132.9, 140.2, 141.5, 149.8, 152.5, 158.4. Anal. calcd. For $C_{13}H_{15}N_5S$: C 57.12, H 5.53, N 25.62%; found: C 57.01, H 5.42, N 25.55 %.

5-(Cyclohexylamino)-6-(pyridin-4-yl)imidazo[2,1-b][1,3,4]thiadiazole (3d): M.p. 138-140°C. IR (KBr) (ν_{max} cm^{-1}):. 3310, 3055, 2950, 2930, 1585, 1530, 1490, 1470, 1420, 1350, 1050, 905, 720, 645. ^{1}H NMR (DMSO-d^6) δ (ppm): 1.21-1.85 (m, 10H, CH_2), 2.56-2.75 (m, 1H), 4.70 (Br s, 1H, NH), 7.90-8.92 (m, 5H, ArH). ^{13}C NMR (DMSO-d^6) δ (ppm): 24.6, 25.3, 34.5, 56.6, 121.5, 133.2, 140.2, 141.5, 149.8, 152.8, 158.3. Anal. calcd. For $C_{15}H_{17}N_5S$: C 60.18, H 5.72, N 23.39%; found: C 60.10, H 5.66, N 23.33 %.

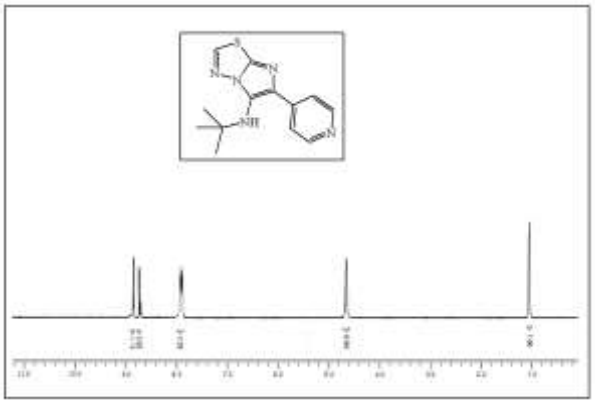

^{1}H-NMR of 3(c)

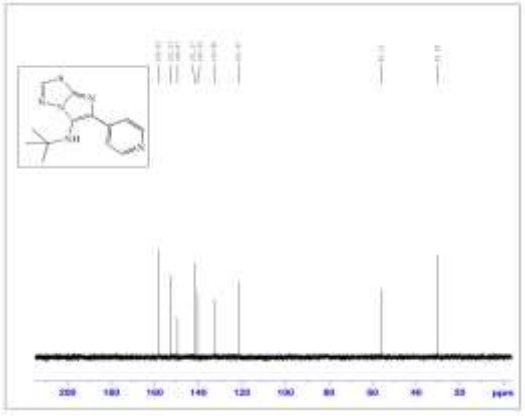

^{13}C-NMR of 3(c)

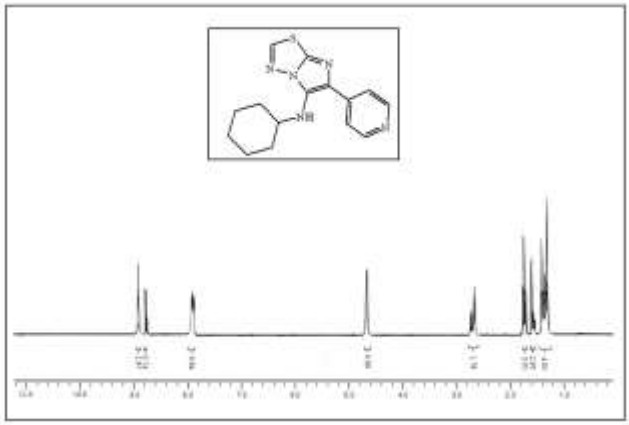

^{1}H-NMR of 3(d)

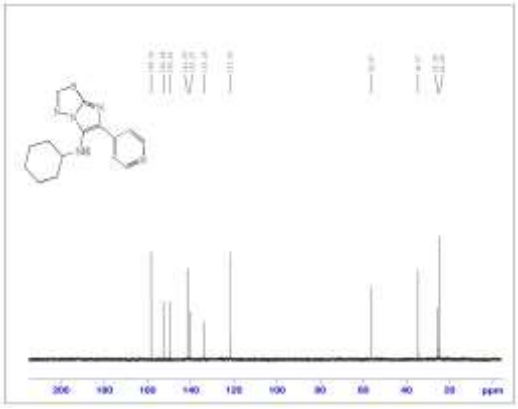

^{13}C-NMR of 3(d)

CONCLUSION

In conclusion, an $MgCe_{0.4}Er_{0.6}FeO_4$ nanoparticle-catalyzed GBB protocol has been developed for the preparation of imidazo[2,1-b][1,3,4]thiadiazole derivatives through a Groebke–Blackburn–Bienaymé annulation . The reaction proceeds under mild conditions and provides structurally diverse broad range products in excellent yields. The heterogenous nanocatalyst offers several advantages, including high catalytic efficiency, facile recovery, and good recyclability. The enhanced catalytic performance $MgCe_{0.4}Er_{0.6}FeO_4$ NPs can be attributed to the accessible active sites and modified surface properties arising from lanthanide doping. Furthermore, the heterogeneous nature of the catalyst facilitates its separation and reuse, making this methodology attractive from both synthetic and sustainability perspectives. Overall, the present approach provides a practical and greener platform for the construction of biologically relevant heterocyclic frameworks through multicomponent synthesis.

References

(a) A.G. Neo, C.F. Marcos. In: M. Giustiniano (Ed.), *Reactive Intermediates in Isocyanide-based Multicomponent Reactions*, Chapter 14. Wiley, 2026. DOI: 10.1002/9783527853793.ch14. (b) A. Domling, I. Ugi, *Angew Chem Int Ed* 2000, 39 3168; (c) C. Hulme, V. Gore, *Curr Med Chem,* 2003, 10 51; (d) I. Ugi, *Angew Chem Int Ed Engl* 1962, 1, 8.

1. (a) M.T. Nazeri, T. Nasiriani, M. Norouzi, S. Torabi, M.A. Vakili, A. Shaabani. *Org. Chem. Front*. 2026. DOI: 10.1039/D6QO00608F; (b) C. Divyavani, P. Padmaja, P. N. Reddy. Curr. Org. Synth. 2024, 21, 140–165; (b) A. Sehlinger, B. Verbraeken, M. A. R. Meier and R. Hoogenboom, *Polym. Chem.*, 2015,6, 3828-3836; (c) (b)G. Koopmanschap, E, Ruijter and R.V.A. Orru, *Beilstein J. Org. Chem.,* 2014, 10, 544–598; (d) C. Che, S. Li, Z. Yu, F. Li, S. Xin, L. Zhou, S. Lin and Z. Yang, *ACS Comb. Sci.,* 2013, 15, 202-207; (e) R. Akbarzadeh, T. Amanpour and A. Bazgir, *Tetrahedron*, 2014, 70, 8142-8147.
2. (a) U. K. Sharma, N. Sharma, D. D. Vachhani and E. V. Van der Eycken, Chem. Soc. Rev., 2015,44, 1836-1860; (b) N. Sharma , Z. Li , U. K. Sharma and E. V. Van der Eycken, *Org. Lett.*, 2014, 16, 3884–3887; (c) A. Kumar, Z. Li, S. K. Sharma, V. S. Parmar and E. V. Van der Eycken *Org. Lett.*, 2013, 15,1874–1877; (d) D. D. Vachhani, A. Kumar, S. G. Modha, S. K. Sharma, V. S. Parmar and E. V. Van der Eycken *Synthesis,* 2015, 47, 1337-1347.
3. (a) S. Schauermann, N. Nilius, S. Shaikhutdinov and H. J. Freund, *Acc. Chem. Res.*, 2013, 46, 1673–1681; (b) J. Liu, L. Chen, H. Cui, J . Zhang, L. Zhang and C.Y. Su, *Chem. Soc. Rev.*, 2014,43, 6011-6061; (c) M. B. Gawande, P. S. Branco and R. S. Varma, *Chem. Soc. Rev.*, 2013,42, 3371-3393; (d) P. Hervés, M. P. Lorenzo, L. M. Liz-Marzán, J. Dzubiella, Y. Lu and M. Ballauff, *Chem. Soc. Rev.*, 2012,41, 5577-5587; (e) B. R. Cuenya, *Thin Solid Films,* 2010, 518 3127–3150
4. (a) C. Sanchez, B. Julián, P. Belleville and M. Popall, ***J. Mater. Chem.***, 2005, **15**, 3559-3592; (b) S. Kango, S. Kalia, A. Celli, J. Njuguna, Y. Habibi and R. Kumar *Progress in Polymer Science,* 2013, 38, 1232–1261; (c) P. Herves, M. P. Lorenzo, L. M. Liz-Marzan, J. Dzubiella, Y. Lu and M. Ballauff, *Chem. Soc.Rev.*, 2012, 41, 5577-5587; (j) B. S. Takale, M. Bao and Y. Yamamoto, *Org. Biomol. Chem.,* 2014, 12, 2005-2027.

5. (a) S. Santra, A. K. Bagdi, A. Majee and A. Hajra, *RSC Adv.*, 2013, 3, 24931; (b) a) J. Safari and Z. Zarnegar, *Ultrasonics Sonochemistry,* 2014, 21, 1132–1139; (b) J. K. Rajput and G. Kaur , *Catal. Sci. Technol.*, 2014, 4, 142-151; (c) J. Safaei-Ghomi, M. A. Ghasemzadeh and M. Mehrabi, *Scientia Iranica,* 2013, 20, 549-554.

6. N.S. Anjos, D.P. Marques, S.J. Coutinho, F.S.F. Borges, A. Santos, P. Licence, L.S. Longo Jr. ACS Omega 2026, 11, 39204–39217. DOI: 10.1021/acsomega.6c03507; (a) A. Shaabani, E. Soleimani, A. Sarvary, A. H. Rezayan and A. Maleki, *Chin. J. Chem.,* 2009, 27, 369; (b) D. Singh, S. Sharma , R. K. Thakur, Vaishali, S. N. Jyoti, C. C. Malakar, V. Singh *Tetrahedron* 152 (2024) 133809; (c) A. Shaabani, A. Maleki, J. Rad and E. Soleimani, *Chem. Pharm.,* 2007, 55, 957; (d) N. Devi, D. Singh, Honey, S. Mor, S. Chaudhary, R.K. Rawal, V. Kumar, A. K Chowdhury, V. Singh, RSC Adv. 6 (2016) 43881; (e) N. Devi, G. Kaur, D. Singh, S. Mor, V.P.R.K. Putta, S. Polina, C.C. Malakar, V. Singh, New J. Chem. 41 (2016) 1082; (f) N. Devi, D. Singh, R.K. Sunkaria, C.C. Malakar, S. Mehra, R.K. Rawal, V. Singh, ChemistrySelect 1 (2016) 4696; (g) S. Sharma, A. Kumar Paul, V. Singh, New J. Chem. 44 (2020) 684; (h) S. Rostamnia and A. Hassankhani, *RSC Adv.,* 2013, 3, 18626; (i) A. H. Shinde, M. Srilaxmi, B. Satpathi, D. S. Sharada, *Tetrahedron Lett.,* 2014, 55, 5915-5920; (j) A. L. Rousseau, P. Matlaba and C. J. Parkinson, *Tetrahedron Lett.,* 2007, 48, 4079; (k) S. K. Guchhait and C. Maadan, Synlett, 2009, 628.

7. K. Aghaie, K. Amiri, M. Rezaei-Gohar, F. Rominger, D. Dar'in, A. Sapeginc, S. Balalaie. *Chem. Commun*. 2024, 60, 2661–2664; (b) A. Shaabani, F. Rezazadeh, E. Soleimani, *Monatsh Chem.,* 2008, 139, 931–933; 28 (c) C. Blackburn, *Tetrahedron Lett.,* 1998, 39, 5469; (d) H. Bienayme and K. Bouzid, *Angew. Chem., Int. Ed.,* 1998, 37, 2234; (e) C. Che, J. Xiang, G. Wang, R. Fathi, J. Quan, Z. Yang, *ACS Comb Sci*., 2007, 9, 982–989; (f) A, Shaabani, E. Soleimani, A. Maleki, *Monatsh Chem*., 2007, 138, 73–76.

8. A.K. Gadad, M.B. Palkar, K. Anand, M.N. Noolvi, T.S. Boreddy, J. Wagwade. Bioorg. Med. Chem. 2008, 16, 276–283; (b) A.K. Gadad, M.B. Palkar, K. Anand, M.N. Noolvi, T.S. Boreddy, J. Wagwade. Bioorg. Med. Chem. 2008, 16, 276–283; (c) I. A. M. Khazia, A. K. Gadadb, R. S. Lamania, B. A. Bhongade, *Tetrahedron* 2011, 67, 3289-331 (d) B. A. Bhongade, S. Talath, R. A. Gadad, A. K. Gadad, *Journal of Saudi Chemical Society*, 2013; (e) A. S. Shawali, *Journal of Advanced Research*, 5, 2014, 1–

17; (f) I. A. M. Khazi, A. K. Gadad, R. S. Lamani, B. A. Bhongade, *Tetrahedron* 2011, 67, 3289-3316.

9. P. Hu, T. Chang, W. Chen, J. Deng, S. Li, Y. Zuo, L. Kang, F. Yang, M. Hostetter, A.A. Volinsky. J. Alloys Compd. 2018, 739, 1–19.
10. N.J. Tang, W. Zhong, H.Y. Jiang, X.L. Wu, W. Liu, Y.W. Du. J. Magn. Magn. Mater. 2004, 282, 92–94.
11. V.J. Angadi, L. Choudhury, K. Sadhana, H. Liu, R. Sandhya, S. Matteppanavar, B. Rudraswamy, V. Pattar, R.V. Anavekar, K. Praveen. J. Magn. Magn. Mater. 2017, 424, 1–11.